Original Research

HCAR2 Exerts Anti-Depressive Effects on Corticosterone-Induced Depression in Mice by Modulating Microglial Activity

Zhao Pan[1],[†], Li Jiang[1],[†], Jiacheng Chen[2], Sicong Xu[1], Ping Zhang[1], Yili Yi[1], Yangzhi Xie[1],*, Yongjun Chen[1],*

[1]Department of Neurology, The Affiliated Nanhua Hospital, Hengyang Medical School, University of South China, 421001 Hengyang, Hunan, China
[2]Department of Intensive Care Unit, The Affiliated Nanhua Hospital, Hengyang Medical School, University of South China, 421001 Hengyang, Hunan, China
*Correspondence: yangtzexie_usc@126.com (Yangzhi Xie); chenyj-usc@foxmail.com (Yongjun Chen)
[†]These authors contributed equally.

Abstract

Background: The metabolites derived from judicious dietary choices play a crucial role in the management and treatment of depression. Hydroxy-carboxylic acid receptor 2 (HCAR2) functions as a receptor for various diet-derived metabolites. Although a growing body of evidence indicates these metabolites exert beneficial effects on depression, the precise mechanisms underlying these benefits require further investigation. **Methods**: We established a mouse model of corticosterone (Cor)-induced depression to evaluate the therapeutic potential of HCAR2 activation on depression. A series of behavioral experiments were conducted to investigate whether HCAR2 activation could alleviate depressive-like behaviors in mice. The neuroprotective effects of HCAR2 in the hippocampus were examined using Nissl and hematoxylin-eosin (HE) staining. The levels of monoamine neurotransmitters in mouse serum were quantified, as well as the cell viability and lactate dehydrogenase (LDH) activity of hippocampal neurons co-cultured with primary microglia. Microglia-associated neuroinflammation was evaluated by quantifying pro-inflammatory cytokines using ELISA, and by assessing the polarization state of M1 microglia, including the mRNA expression levels of M1 markers and double fluorescence staining for inducible nitric oxide synthase/ionized calcium-binding adapter molecule 1 (iNOS/Iba1). The expression level of proteins in the protein kinase B-inhibitor of nuclear factor kappa-B kinase subunits alpha and beta-nuclear factor kappa-light-chain-enhancer of activated B cells (AKT-IKK$\alpha\beta$-NFκB) pathway in primary microglia was analyzed using western blot. Transcriptomic changes in microglia induced by HCAR2 activation were examined through RNA sequencing. Mice were fed PLX5622 chow to deplete microglia *in vivo*. **Results**: Activation of HCAR2 by its agonist MK-6892 in a Cor-induced model of depression significantly alleviated depressive-like behaviors, attenuated hippocampal neuronal injury, increased serum monoamine levels, reduced microglia-associated neuroinflammation, and inhibited the expression of proteins in the AKT-IKK$\alpha\beta$-NFκB pathway in primary microglia. Additionally, HCAR2 activation markedly enhanced hippocampal neuronal viability and decreased LDH activity in this co-culture system. Importantly, these protective effects were abolished in HCAR2 knockout mice. RNA sequencing revealed that HCAR2 activation induced changes in multiple signaling pathways. Moreover, the depletion of microglia also eliminated the protective effects of MK-6892. **Conclusion**: Activation of HCAR2 can reduce depressive-like behaviors, neuronal injury, and neuroinflammation. Our findings suggest these neuroprotective effects are, at least in part, mediated through modulation of microglial activity by HCAR2.

Keywords: depression; HCAR2; microglia; neuroinflammation

1. Introduction

Major depressive disorder (MDD) is a psychiatric condition characterized by pervasive and persistent feelings of sadness, anhedonia, and diminished interest in activities that were previously pleasurable [1]. The etiology of MDD remains largely unclear. Furthermore, depression represents a highly heterogeneous diagnostic category. Despite the well-documented efficacy of antidepressants, approximately 20% to 30% of patients with clinical depression show either no response, or suboptimal outcomes after receiving standard antidepressant treatment [2]. Therefore, the development of alternative therapeutic approaches for the treatment of depression is a major imperative. Nu-

merous studies have demonstrated that metabolites generated from prudent dietary selections can exert beneficial effects on individuals suffering from depression [3,4]. For instance, it has been shown that fish rich in omega-3 fatty acids, dairy products and shiitake mushrooms containing high tryptophan and tyrosine levels, and animal liver and egg yolks with abundant vitamins D and B can serve as effective adjuncts in the clinical treatment of depression. Hydroxy-carboxylic acid receptor 2 (HCAR2) is a G-protein-coupled receptor that can be activated by beta-hydroxybutyric acid, butyrate, and niacin [5]. These metabolites have demonstrated a substantial capacity to attenuate the progression of depression [6–8], suggesting that
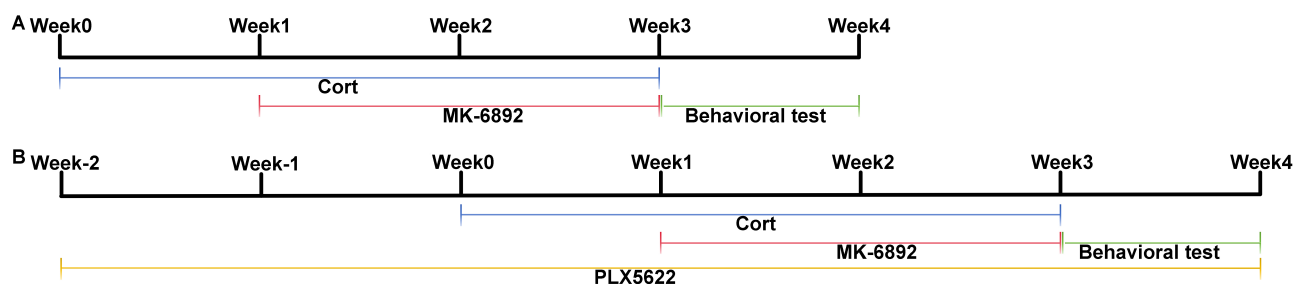
Fig. 1. Experimental timeline utilized in this study. (A) Timeline for assessing the therapeutic effects of HCAR2 activation in a murine model of depression. (B) Timeline for assessing the therapeutic effects of HCAR2 activation following microglia depletion in a murine model of depression. HCAR2, hydroxy-carboxylic acid receptor 2.

HCAR2 may serve as a promising therapeutic target for the treatment of this condition. However, the precise mechanism through which HCAR2 exerts its antidepressant effects remains to be elucidated.

Microglia function as the primary immune cells in the central nervous system (CNS). They are responsible for surveilling the local environment and executing diverse roles, including phagocytosis of cellular debris, promotion of neurogenesis, synaptic pruning, and secretion of cytokines and chemokines [9]. Previous autopsy study has shown that expression levels of inflammatory factors in the brains of patients with depression were significantly elevated compared to the control group [10]. Additionally, a marked increase in the mRNA expression level of Toll-like receptor 3 (TLR3), Toll-like receptor 4 (TLR4), and Toll-like receptor 7 (TLR7) was observed specifically within the prefrontal cortex (PFC) [11]. This finding suggests that patients with MDD have elevated microglial density and activation. Inhibition of microglial inflammatory signaling has been demonstrated to improve treatment outcomes in MDD. Minocycline is an anti-inflammatory antibiotic that effectively suppresses inflammatory activation in microglia and exhibits antidepressant properties in MDD patients and in a rodent model of depression [12,13]. The overactivation of microglia is intricately linked to neuronal impairment in the pathology of MDD. Consequently, the modulation of microglial inflammation represents a promising therapeutic strategy for managing depression.

The aim of this study was therefore to investigate the role of HCAR2 in a rodent model of depression. We hypothesize that the therapeutic potential of HCAR2 may be associated with its ability to modulate microglial activity.

2. Methods

2.1 Animals and Grouping

All animal experiments were conducted in strict compliance with the guidelines for laboratory animal care and utilization established by the National Institutes of Health. Wild-type (WT) and HCAR2 knockout (KO) C57BL/6 mice (6–8 weeks old, strain NO. T006705) were purchased from Gempharmatech (Nanjing, Jiangsu, China)

and housed under standard laboratory conditions. They were given *ad libitum* access to water and food and maintained on a 12-h light/12-h dark cycle. Mice were intraperitoneally administered with a daily dose of corticosterone (Cor, 20 mg/kg, 50-22-6, Aladdin, Shanghai, China) for a continuous three-week period to establish a rodent model of depression. To evaluate the therapeutic effects of HCAR2 activation in this model, mice were then randomly assigned to one of four groups for a two-week treatment period: a control group (administered saline), a Cor group, an HCAR2 agonist (MK-6892, HY-10680, MedChemExpress, Monmouth Junction, NJ, USA) group, and a combined Cor+MK-6892 group (Fig. 1A). To investigate whether the antidepressant and neuroprotective effects of HCAR2 activation were mediated through its action on microglia, mice were administered PLX5622 chow (PLX, HY-114153, Monmouth Junction, NJ, USA) throughout the experimental period to deplete microglia *in vivo*. AIN-76A chow (Shanghai Yubo Bio-technology Co., Ltd.02960097-CF, Shanghai, China) served as the vehicle (Veh) control in this study. Mice were randomly assigned to one of three groups: Cor+MK-6892, Cor+Veh+MK-6892, or Cor+PLX+MK-6892 (Fig. 1B). Behavioral tests were conducted within one week following the completion of drug treatment. The mice were then anesthetized with a mixture of xylazine (7361-61-7; Merck, Rahway, NJ, USA; 10 mg/kg, i.p.) and ketamine (H20023609; Jiuxu Pharmaceutical Co., Ltd., Jinhua, Zhejiang, China; 90 mg/kg, i.p.), after which samples were collected for subsequent analyses. In particular, a volume of 2 μL of MK-6892 (100 mg/kg) or saline was administered via intracerebroventricular infusion. Mice were euthanized using gradual CO_2 inhalation. CO_2 was introduced into a transparent chamber at a flow rate displacing 20% of the chamber volume per minute until the final CO_2 concentration exceeded 70%. After confirming respiratory arrest, this concentration was maintained for an additional 5 minutes to ensure death.

2.2 Behavioral Tests

The mice underwent a battery of behavioral tests designed specifically to evaluate depression-like behaviors.

IMR Press

For the tail suspension test, the tail was gently secured to the tail hanger, ensuring the animal's head was positioned downward, with a distance of approximately 30 cm maintained from the bottom of the hanger. Following the adaptation period, the duration of immobility was measured during a 4-minute interval. For the forced swimming test, the water temperature in the test chamber was adjusted to a range of 23–25 °C prior to commencing the experiment. Mice were acclimatized to swimming one day before the experiment. At 24 h after the acclimatization period, the length of time of immobility was recorded over a period of 5-minute duration. For the sucrose preference test, mice were first acclimatized to sucrose water over a 24-h adaptation period. Specifically, each rat was provided with two bottles: one containing 1% sucrose solution (wt/vol) and the other containing purified water. The bottles were randomly positioned on either the right or left side of each cage. To control for position bias, the position of each bottle was switched after 12 h. The sucrose preference test was conducted after this adaptation period. Following baseline measurements, the mice underwent a 24-h period of food and water deprivation. Thereafter, they were promptly subjected to a 12-h sugar preference test. For the open field test, mice were placed in a square arena measuring 1×1 meter. After a period of acclimatization, the frequency of rearing behavior was recorded during a 4-minute observation period.

2.3 Hematoxylin-Eosin Staining

The sample was fixed in a solution of 95% ethanol and ice-cold acetone for 20 minutes, and subsequently rinsed twice with phosphate-buffered saline (PBS) to remove residual fixative. The samples were then stained with hematoxylin solution for 2–3 minutes to visualize the nuclei, followed by thorough rinsing with deionized water to ensure complete removal of excess stain. Next, the samples were immersed in eosin solution for 1 minute to stain the cytoplasm, followed by rinsing with deionized water. After air drying, the coverslips were mounted using neutral mounting medium. Observations and photographic documentation were performed 24 h later using an inverted laser confocal microscope (FV1200MPE-share, Olympus, Tokyo, Japan).

2.4 Nissl's Staining

Fresh tissues were fixed in 10% neutral buffered formalin for 48 h, followed by routine dehydration and embedding procedures. The tissues were sectioned into 6–8 µm thick slices, dewaxed, and rinsed multiple times with distilled water. Sections were then immersed in toluidine blue solution and incubated in a thermostat (FP89-HL, Julabo, Seelbach, Germany) maintained at 50–60 °C for 25–50 minutes to ensure optimal staining. After rinsing with distilled water, sections underwent a stepwise dehydration process using ethanol. Xylene was subsequently used for clarification, and the specimens mounted using a neutral mounting medium.

2.5 Enzyme-Linked Immunosorbent Assay (ELISA) and Lactate Dehydrogenase (LDH) Release Assay

ELISA was used to quantify the serum concentrations of 5-hydroxytryptamine (5-HT, EEL006, Invitrogen, Carlsbad, CA, USA) and noradrenaline (NA, EEL010, Invitrogen, Carlsbad, CA, USA) as recommended by the manufacturer of the commercially available kits. ELISA was also used to measure the concentrations of interleukin-1β (IL-1β, PI301, Beyotime, Shanghai, China), interleukin-6 (IL-6, PI326, Beyotime, Shanghai, China), and tumor necrosis factor-α (TNF-α, PT512, Beyotime, Shanghai, China) in primary microglia. LDH activity in primary hippocampal neurons was measured using a commercially available kit (C0018M, Beyotime, Shanghai, China).

2.6 Isolation and Culture of Primary Microglial Cells

Primary microglial cells were isolated using a discontinuous Percoll density gradient centrifugation method as described previously [14]. Briefly, the skull was carefully removed to extract brain tissue, which was then mechanically dissociated. To this homogenate was added 10 mL of sterile $1\times$ DPBS containing 0.2% glucose. The resulting suspension was filtered through a 70 µm nylon cell strainer (CLS431752, Corning, NY, USA) and transferred to a 50 mL centrifuge tube (CLS352099, Corning, NY, USA). Cell suspensions were centrifuged through Percoll gradients, and the cell populations harvested from the interface between the 70% and 50% Percoll layers. The isolated cells were examined after immunofluorescence staining. Primary microglial cells and the mouse hippocampal neuronal cell line HT-22 were cultured in DMEM/F12 medium supplemented with 1% Penicillin/Streptomycin solution and 10% fetal bovine serum. Both cell lines were validated by STR profiling and tested negative for mycoplasma.

2.7 Cell Counting Kit-8 (CCK8)

The CCK8 assay was utilized to evaluate cell viability. Primary hippocampal neurons were seeded into a 96-well plate. After an appropriate attachment period, 10 µL of CCK-8 solution (C0037, Beyotime, Shanghai, China) was added to each well, followed by incubation for 4 h at 37 °C in a humidified 5% CO_2 atmosphere. The absorbance at 450 nm was subsequently measured using a microplate reader (ELx800, BioTek, Santa Clara, CA, USA).

2.8 Immunofluorescent Staining

After routine dewaxing, antigen retrieval, and inactivation, the tissue sections were prepared at a thickness of 5 µm. The sections were incubated in a solution containing 0.2% Triton X-100 at room temperature for 20 minutes, followed by three 5-minute washes with phosphate-

buffered saline with Tween-20 (PBST). Next, the samples were completely covered with a 5% bovine serum albumin (BSA) solution and incubated at room temperature for 30–60 minutes to block non-specific binding sites. After adding the appropriate primary antibody (ionized calcium-binding adapter molecule 1, Iba1, 1:100, ab283319, Abcam, Cambridge, UK), the sections were incubated overnight at 4 °C, then rinsed several times with PBS and incubated with horseradish peroxidase (HRP)-conjugated anti-mouse IgG secondary antibodies. Subsequently, an appropriate volume of tyramide signal amplification (TSA) dye was added and the sections incubated at room temperature in the dark for 10 minutes. Unbound antibodies were eluted using antibody elution buffer, followed by re-blocking with 5% BSA. An optimal concentration of primary antibodies (inducible nitric oxide synthase, iNOS, 1:100, ab210823, Abcam, Cambridge, UK; HCAR2, 1:100, AHR-012, Alomone labs, Jerusalem, Israel) was then added and incubated overnight at 4 °C. The sections were subsequently incubated with HRP-conjugated anti-rabbit IgG secondary antibodies and the TSA dye reapplied, ensuring the fluorescent color differed from that used in the initial staining. Finally, the sections were mounted using an anti-fade mounting medium, examined under a fluorescence microscope, and the images recorded.

2.9 Real-Time Fluorescent Quantitative PCR

TRIzol reagent (15596018CN, Sigma-Aldrich, St. Louis, MO, USA) was used to isolate total RNA, which was then reverse transcribed into cDNA using the Prime-Script RT reagent kit (RR037A, Takara, Kusatsu, Japan). Real-time PCR was performed on a 7300 Plus Real-Time PCR System (JM1966-018481, Thermo Fisher, Waltham, MA, USA) with SYBR Premix Ex Taq I (RR037A, Takara, Kusatsu, Japan). Each reaction mixture comprised 1 µL of cDNA template, 10 µL of PCR master mix, 5 pmol of each primer, and nuclease-free water to a final volume of 20 µL. The thermocycling conditions consisted of an initial denaturation at 95 °C for 13 s, followed by 40 cycles of 94 °C for 10 s, and 60 °C for 20 s. Relative mRNA expression levels were normalized to Glyceraldehyde-3-phosphate dehydrogenase (GAPDH) mRNA as the internal control. Data analysis was conducted using the comparative threshold cycle ($\Delta\Delta$Ct) method. Primer sequences are listed in Table 1.

2.10 Western Blotting

Cells were lysed with radioimmunoprecipitation assay (RIPA) buffer containing phenylmethylsulfonyl fluo-

ride (PMSF). The extracted proteins were separated by 10% sodium dodecyl sulfate–polyacrylamide gel electrophoresis (SDS-PAGE) and subsequently transferred to polyvinylidene fluoride (PVDF) membranes via electroblotting. The membranes were blocked for 1 h at room temperature and then incubated overnight at 4 °C with primary antibodies against phosphorylated protein kinase B (p-AKT, #4060, Cell Signaling Technology, Danvers, MA, USA), total protein kinase B (total-AKT, #4691, Cell Signaling Technology, Danvers, MA, USA), phosphorylated inhibitor of nuclear factor-kappa-B kinase subunits alpha and beta (p-IKK$\alpha\beta$, #2697, Cell Signaling Technology, Danvers, MA, USA), total inhibitor of NFκB kinase subunits alpha and beta (total-IKK$\alpha\beta$, #8943, Cell Signaling Technology, Danvers, MA, USA), phosphorylated nuclear factor kappa-light-chain-enhancer of activated B cells (p-NFκB, #3033, Cell Signaling Technology, Danvers, MA, USA), and total nuclear factor kappa-light-chain-enhancer of activated B cells (total-NFκB, #6956, Cell Signaling Technology, Danvers, MA, USA). After washing, the membranes were incubated with HRP-conjugated secondary antibodies for 1 h at room temperature. The proteins were detected using an enhanced chemiluminescence (ECL) imaging kit (C10637, Thermo Fisher, Waltham, MA, USA), and visualized with a chemiluminescence imaging system (17001402, Bio-Rad, Hercules, CA, USA).

2.11 Comprehensive Analysis of RNA Sequencing

RNA sequencing was carried out through a commercially available service (BGI, the raw sequence data see the availability of data and materials). Briefly, total RNA was fragmented into short fragments and the mRNA enriched using oligo (dT) magnetic beads, followed by cDNA synthesis. Double stranded cDNA was purified and enriched by PCR amplification, after which the library products were sequenced using BGIseq-500. Gene Ontology (GO, http://geneontology.org/docs/download-ontology/) bioinformatics and Kyoto Encyclopedia of Genes and Genomes (KEGG, https://www.kegg.jp/kegg/pathway.html) pathway analyses were performed using the Dr. TOM approach, which is an in-house customized data mining system of the BGI. Altered expression of genes was expressed as log$_2$FC, representing log-transformed fold-change (log$_2$FC = log$_2$[B/A]), where A and B represent the values for gene expression under different treatment conditions.

Table 1. Primer sequences.

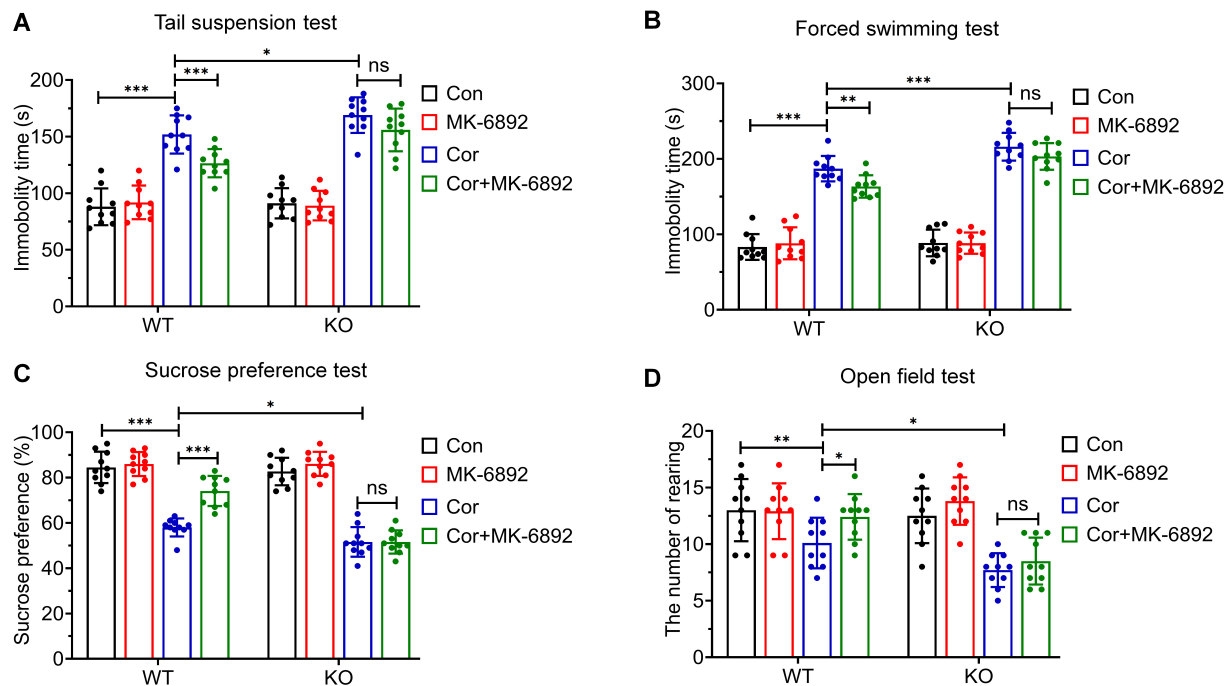| Target gene	Foward primer sequence	Reverse primer sequence
iNOS	GGTGAAGGGACTGAGCTGTT	ACGTTCGTTCTCTTGCA
TNF-α	CAGGCGGTGCCTATGTCTC	CCATTTGGGAACTTCTCATCCCTT
GAPDH	GCCAAGGCTGTGGGCAAGGT	TCTCCAGGCGGCACGCAGA

Fig. 2. Effects of HCAR2 activation on corticosterone-induced depressive behaviors. (A) Immobility time in the tail suspension test. (B) Immobility time in the forced swimming test. (C) Sucrose preference test. (D) Frequency of rearing behavior in the open field test. ***$p < 0.001$, **$p < 0.01$, *$p < 0.05$; ns, not significant; WT, wild type; KO, knock out; Con, control; Cor, corticosterone.

2.12 Statistical Analysis

All data are presented as the mean $\pm$ SEM and were analyzed using one-way Analysis of Variance (ANOVA) followed by Tukey's post hoc test. Statistical analyses were performed using SPSS 22.0 software (IBM Corp., Chicago, IL, USA). A p-value of less than 0.05 was considered statistically significant.

3. Results

3.1 Activation of HCAR2 Alleviates Corticosterone-Induced Depressive Behaviors

To assess whether HCAR2 activation can mitigate corticosterone-induced depressive behaviors, we conducted the following tests across all experimental groups: tail suspension test (TST; Fig. 2A), forced swimming test (FST; Fig. 2B), sucrose preference test (SPT; Fig. 2C), and open field test (OFT; Fig. 2D). In the WT group, MK-6892 treatment significantly reduced corticosterone-induced depressive behaviors (TST: $p < 0.001$; FST: $p < 0.001$; SPT: $p < 0.001$; OFT: $p = 0.005$). Furthermore, HCAR2 KO mice that received corticosterone treatment displayed markedly more severe depressive behaviors compared to WT mice subjected to the identical regimen. (TST: $p = 0.015$; FST: $p < 0.001$; SPT: $p = 0.016$; OFT: $p = 0.018$). In the KO group, no statistically significant difference was observed between the Cor+MK-6892 group and the Cor-only group. These data indicate that HCAR2 activation can significantly alleviate corticosterone-induced depressive behaviors in mice.

3.2 Activation of HCAR2 Mitigates Corticosterone-Induced Neuronal Damage and the Depletion of Monoamine Neurotransmitters

The protective effects of HCAR2 activation in this murine model of depression were investigated by hematoxylin-eosin staining (Fig. 3A) and Nissl staining (Fig. 3C) across all experimental groups. In the WT group, HCAR2 activation in the depression model significantly enhanced the survival of hippocampal neurons, as evidenced by the reduced number of cells exhibiting nuclear pyknosis ($p < 0.001$, Fig. 3B), and decreased the number of injured neurons ($p < 0.001$, Fig. 3D). Moreover, HCAR2 KO mice exhibited more severe neurological impairments following corticosterone administration compared to their WT counterparts under identical treatment conditions ($p = 0.005$, Fig. 3B; $p < 0.001$, Fig. 3D). We next evaluated the serum levels of 5-HT and NA. Activation of HCAR2 significantly reduced the corticosterone-induced depletion of monoamine neurotransmitters in WT mice (5-HT: $p = 0.002$; NA: $p = 0.011$, Fig. 3E). The HCAR2 KO depression model displayed a more pronounced depletion of monoamine neurotransmitters compared to the WT depression model (5-HT: $p = 0.003$; NA: $p < 0.001$, Fig. 3E). The protective effect of MK-6892 was found to be specifically mediated via HCAR2, as no significant difference was observed between the depressive model group and the drug-treated group in KO mice. These data suggest that activation of HCAR2 can markedly reduce corticosterone-induced neuronal injury.
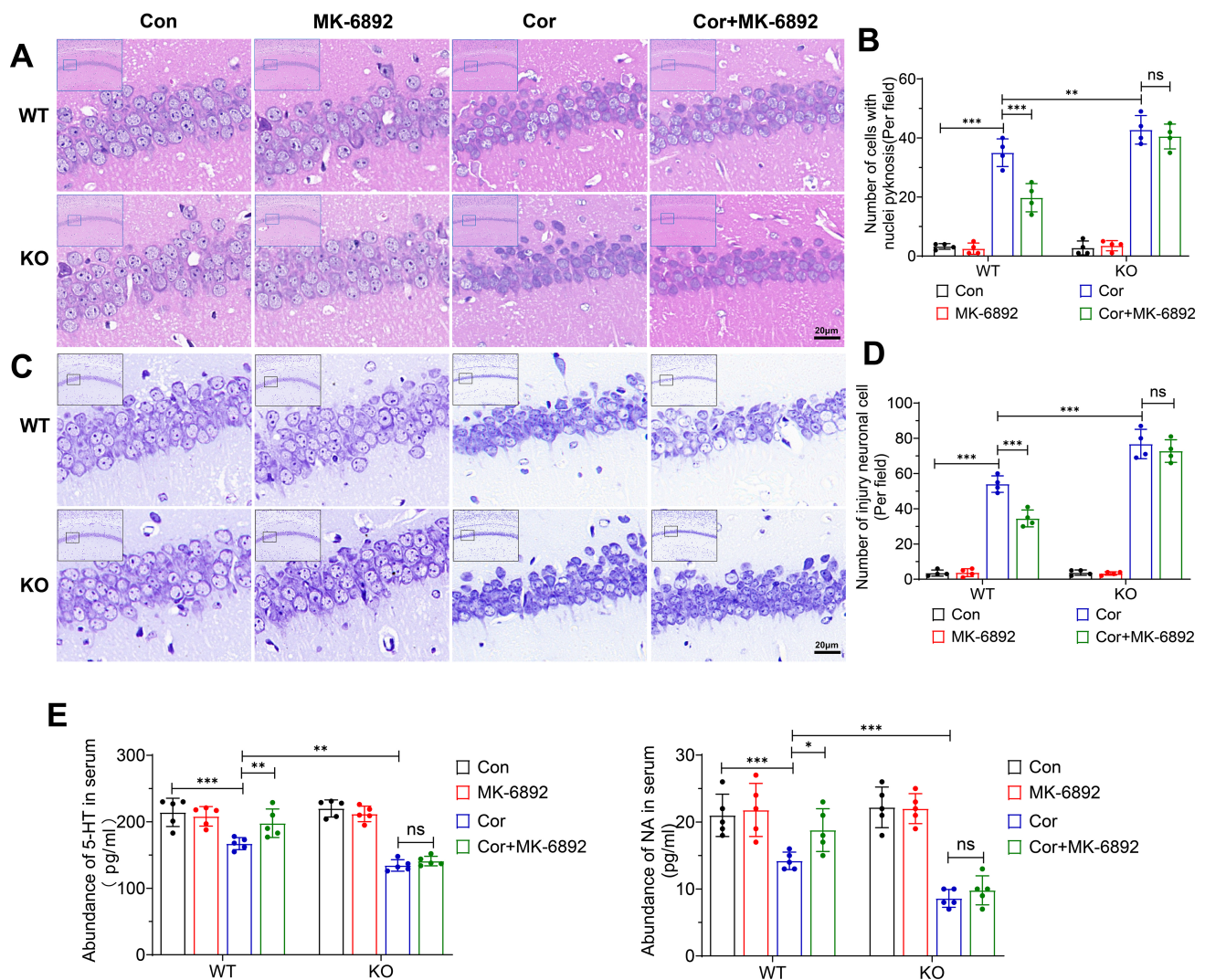
Fig. 3. Effects of HCAR2 activation on corticosterone-induced hippocampal neuronal injury. (A) Representative hematoxylin-eosin stained images of the hippocampus from each experimental group. Scale bar = 20 μm. (B) Bar graph depicting the number of cells exhibiting nuclear pyknosis. (C) Representative Nissl-stained images of the hippocampus from each experimental group. Scale bar = 20 μm. (D) Bar graph showing the number of injured neurons. (E) Serum levels of monoamine neurotransmitter, as measured by ELISA. $***p < 0.001$, $**p < 0.01$, $*p < 0.05$; ns, not significant; WT, wild type; KO, knock out; Con, control; Cor, corticosterone; 5-HT, 5-Hydroxytryptamine; NA, norepinephrine.

3.3 Co-Localization of Iba1 and HCAR2 in Microglial Cells

To confirm the expression of HCAR2 in microglial cells, immunofluorescence staining was conducted on the hippocampus (Fig. 4A) and on primary microglial cells (Fig. 4B). HCAR2 was found to co-localize with Iba1, a marker for microglia, indicating that HCAR2 is expressed in microglial cells.

3.4 Activation of HCAR2 Attenuates Neuronal Injury in a Co-Culture Model

We subsequently examined whether activation of HCAR2 in microglial cells could induce neuroprotective effects on cells from the hippocampal neuron HT-22 cell line

in a co-culture model (Fig. 5A). Primary microglial cells were isolated from the specified experimental groups, and a 0.4 μm pore-sized membrane was used to segregate primary microglial cells from HT-22 cells. After co-culture for 48 h, the cell viability and LDH activity were assessed in each experimental group. HT-22 cells co-cultured with microglia isolated from WT mice and treated with a combination of Cor and MK-6892 were found to exhibit significantly greater cell viability ($p = 0.005$, Fig. 5B) and markedly lower LDH activity ($p < 0.001$, Fig. 5C) compared to HT-22 cells co-cultured with microglia from WT mice treated with Cor alone. Furthermore, HT-22 cells co-cultured with microglia derived from KO mice treated with corticosterone exhibited significantly reduced cell viability and elevated
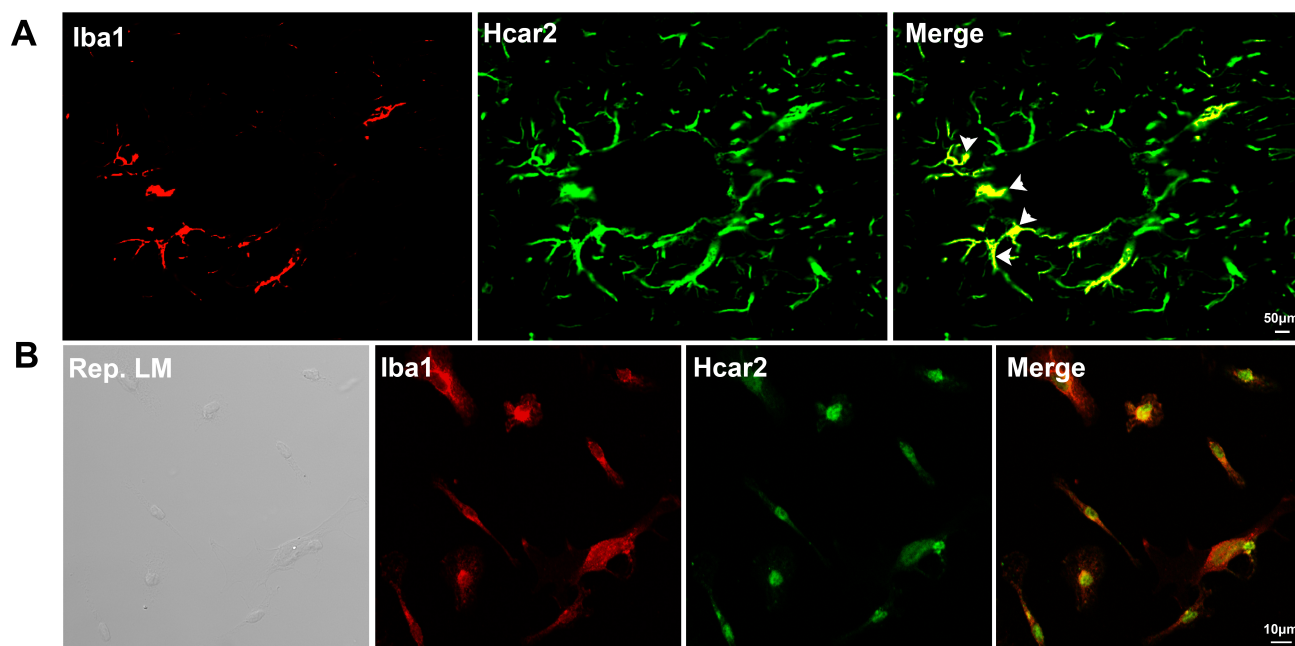
Fig. 4. Co-localization of Iba1 and HCAR2 *in vivo* and *in vitro*. (A) Co-localization of Iba1 and HCAR2 in brain sections. Scale bar = 50 μm. The white arrow indicates the co-localization of Iba1 and HCAR2 within the hippocampal region. (B) Co-localization of Iba1 and HCAR2 in primary microglial cells. Scale bar = 10 μm. Iba1, ionized calcium-binding adapter molecule 1; LM, light microscopy.
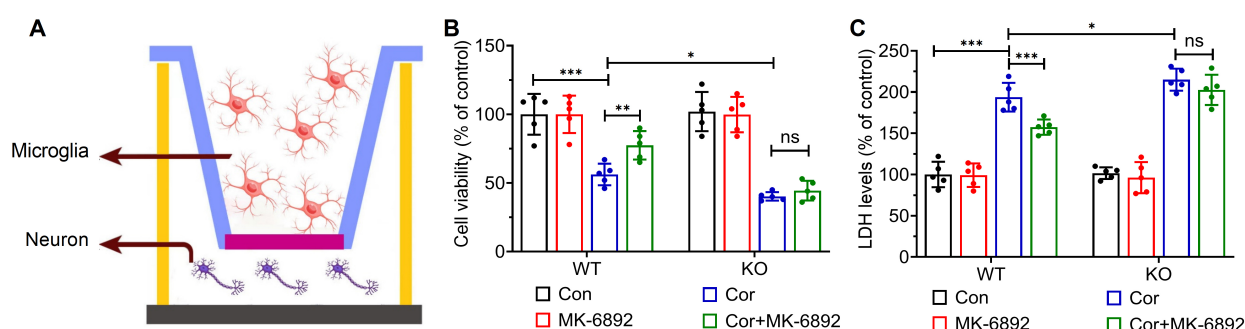

Fig. 5. HCAR2 activation alleviates hippocampal neuronal injury in a co-culture system. (A) Schematic diagram of the co-culture model. This figure was created using Adobe Illustrator software. (B) Cell viability in each experimental group. (C) LDH levels in each experimental group. ***$p < 0.001$, **$p < 0.01$, *$p < 0.05$; ns, not significant; WT, wild type; KO, knock out; Con, control; Cor, corticosterone; LDH, lactate dehydrogenase.

LDH activity compared to HT-22 cells co-cultured with microglia from WT mice under identical treatment conditions. No significant differences were observed between the Cor and Cor+MK-6892 groups within the KO group. These data indicate that activation of HCAR2 in microglia may confer protection against corticosterone-induced neuronal injury *in vitro*.

3.5 Activation of HCAR2 Inhibits Corticosterone-Induced Microglial M1 Polarization

The degree of M1 polarization in microglia was assessed by performing immunofluorescent staining for Iba1/iNOS in the hippocampus (Fig. 6A), as well as real-time qPCR analysis to evaluate the expression lev-

els of iNOS and TNF-α in primary microglia (Fig. 6C). Immunofluorescent staining in WT mice demonstrated a markedly reduced proportion of Iba1/iNOS double-positive microglia in the Cor+MK-6892 group relative to the Cor-only group ($p = 0.004$, Fig. 6B). Consistent with these observations, real-time qPCR analysis in WT mice revealed the Cor+MK-6892 group exhibited markedly reduced levels of microglial M1 phenotype mRNA relative to the Cor-only group (iNOS: $p < 0.001$; TNF-α: $p < 0.001$; Fig. 6C). Furthermore, Cor-treated KO mice displayed a significantly higher degree of M1 polarization relative to Cor-treated WT mice, as indicated by immunofluorescent staining ($p = 0.02$, Fig. 6B) and real-time qPCR analysis (iNOS: $p < 0.001$; TNF-α: $p < 0.001$; Fig. 6C). In KO mice, no statistically
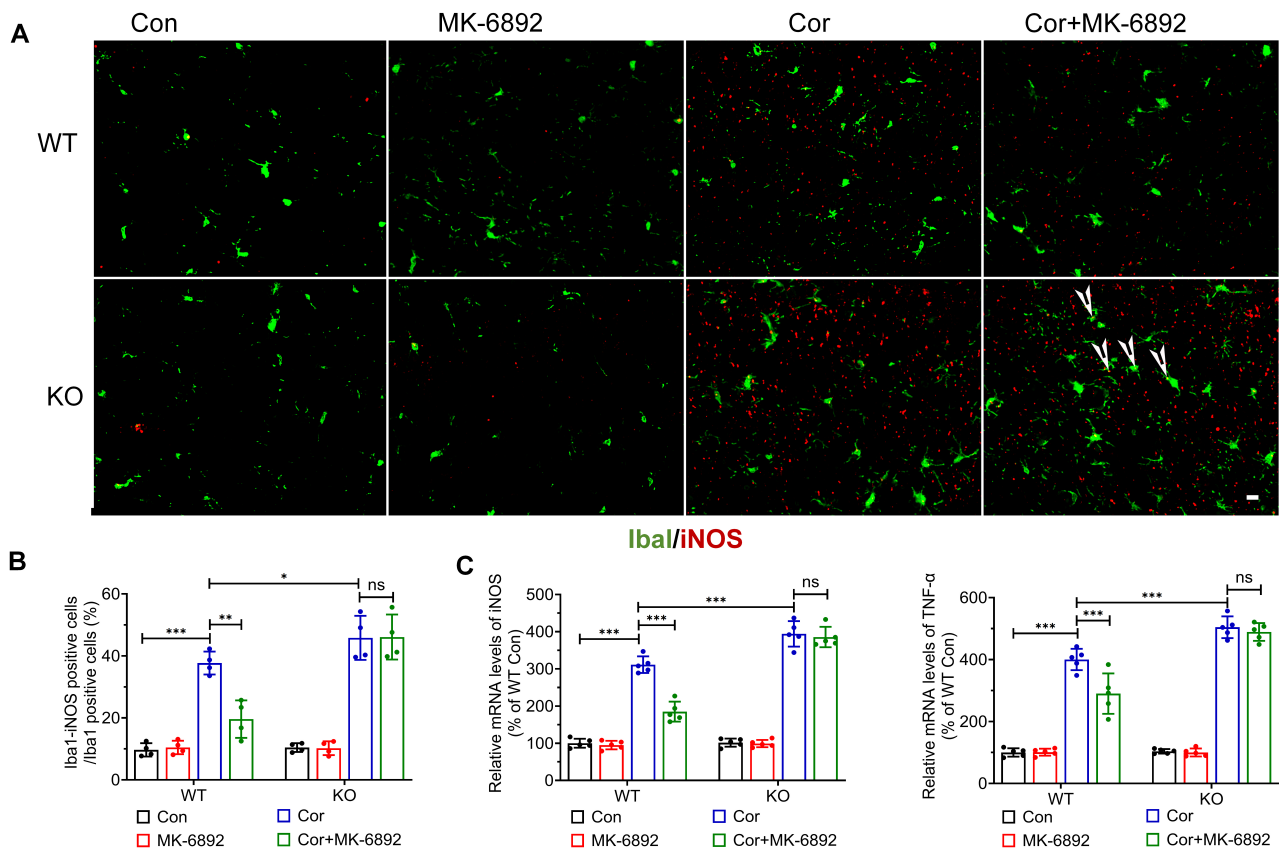
Fig. 6. Activation of HCAR2 inhibits microglial M1 polarization. (A) Representative immunofluorescent staining for Iba1 and iNOS in the hippocampus. Scale bar = 100 μm. The white arrow indicates the co-localization of iNOS and Iba1 within the hippocampal region. (B) Quantification of the number of Iba1/iNOS double-positive microglia. (C) Relative mRNA levels of selected M1 phenotype markers in primary microglia. ***$p < 0.001$, **$p < 0.01$, *$p < 0.05$; ns, not significant; WT, wild type; KO, knock out; Con, control; Cor, corticosterone.

significant difference was observed between the Cor+MK-6892 group and the Cor-only group. These data suggest that HCAR2 is effective at inhibiting microglial M1 polarization.

3.6 Activation of HCAR2 Mitigates Corticosterone-Induced Activation of the AKT-IKKαβ-NFκB Pathway and the Release of Pro-Inflammatory Cytokines in Microglia

Modulation of the protein kinase B-inhibitor of nuclear factor kappa-B kinase subunits alpha and beta-nuclear factor kappa-light-chain-enhancer of activated B cells (AKT-IKKαβ-NFκB) pathway plays a critical role in mitigating inflammatory responses. Consequently, we performed Western blot analysis to examine the role of this pathway on the anti-inflammatory effects induced by HCAR2 (Fig. 7A,E). Corticosterone treatment resulted in significant upregulation of the expression of p-AKT ($p < 0.001$, Fig. 7B), p-IKKαβ ($p < 0.001$, Fig. 7C), and p-NFκB proteins ($p < 0.001$, Fig. 7D), whereas MK-6892 treatment downregulated the expression of these proteins (p-AKT: $p = 0.002$, Fig. 7B; p-IKKαβ: $p < 0.001$, Fig. 7C;

p-NFκB: $p = 0.025$, Fig. 7D) in primary microglia isolated from WT mice. However, no significant difference in protein expression was observed between the Cor+MK-6892 group and the Cor-only group in KO mice (Fig. 7F–H). In addition, the ELISA method was used to quantify the concentrations of selected pro-inflammatory cytokines. Treatment with MK-6892 significantly reduced the release of corticosterone-induced proinflammatory cytokines in microglia from WT mice (IL-1β: $p = 0.02$; IL-6: $p = 0.018$; TNF-α: $p = 0.005$; Fig. 7I–K). Of note, no significant differences were observed between the Cor+MK-6892 group and the Cor-only group in KO mice. These data suggest that activation of HCAR2 can markedly attenuate the inflammatory response.

3.7 Activation of HCAR2 Transcriptionally Regulates Global Gene Expression of Microglia in Cor-Treated Mice

Comprehensive profiling of HCAR2-mediated transcriptional regulation in the brain was performed by extracting total RNA from microglia isolated from both Cor-treated and Cor+MK-6892-treated WT mice. This was fol-
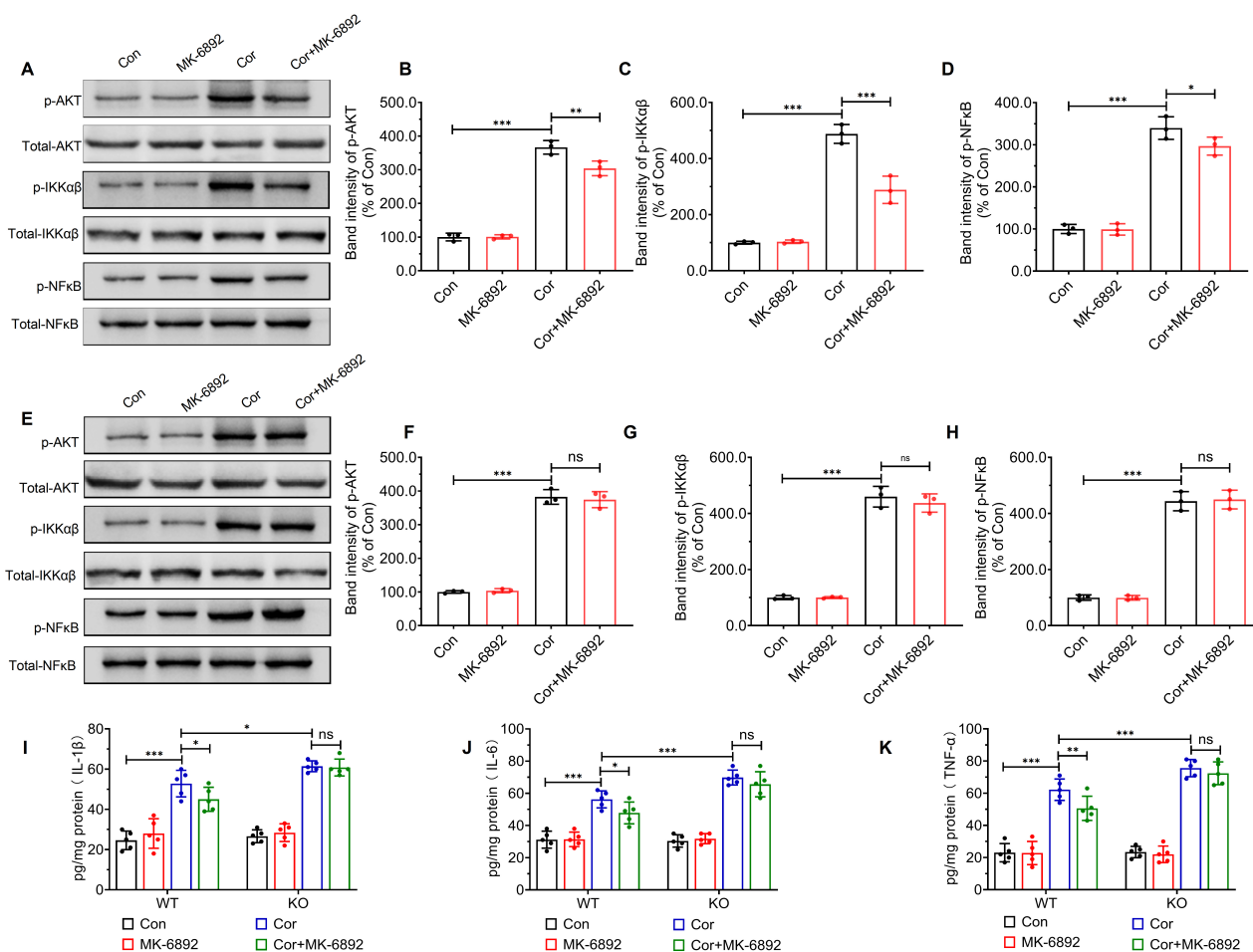
Fig. 7. HCAR2 activation inhibits corticosterone-induced activation of the AKT-IKK$\alpha\beta$-NFκB pathway in primary microglial cells. (A) Immunoblot analysis of p-AKT, p-IKK$\alpha\beta$, and p-NFκB protein expression in primary microglial cells isolated from WT mice. (B–D) Quantitative bar graphs representing relative protein levels of p-AKT, p-IKK$\alpha\beta$, and p-NFκB in primary microglial cells from WT mice. (E) Immunoblot analysis of p-AKT, p-IKK$\alpha\beta$, and p-NFκB protein expression in primary microglial cells isolated from KO mice. (F–H) Quantitative bar graphs representing relative protein levels of p-AKT, p-IKK$\alpha\beta$, and p-NFκB in primary microglial cells from KO mice. (I–K) Quantification of pro-inflammatory cytokine levels using ELISA. ***$p < 0.001$, **$p < 0.01$, *$p < 0.05$; ns, not significant; WT, wild type; KO, knock out; Con, control; Cor, corticosterone; p-AKT, phosphorylated protein kinase B; p-IKK$\alpha\beta$, phosphorylated inhibitor of nuclear factor-kappa-B kinase subunits alpha and beta; p-NFκB, phosphorylated nuclear factor kappa-light-chain-enhancer of activated B cells; total-AKT, total protein kinase B; total-IKK$\alpha\beta$, total inhibitor of NFκB kinase subunits alpha and beta; total-NFκB, total nuclear factor kappa-light-chain-enhancer of activated B cells; IL, interleukin; TNF-α, tumor necrosis factor-alpha.

lowed by high-throughput sequencing and bioinformatic analysis. Heat map analysis of differential gene expression identified 174 differentially expressed genes (DEGs) between the Cor and Cor+MK-6892 groups, comprising 64 upregulated genes and 110 downregulated genes (Fig. 8A). KEGG analysis (Fig. 8B) revealed that HCAR2 activation in microglia primarily regulated genes associated with metabolic pathways (tryptophan metabolism, purine metabolism, etc.) and cellular processes (cell adhesion molecule, neutrophil extracellular trap formation, etc.). Gene Ontology enrichment analysis (Fig. 8C) revealed that microglia from the Cor+MK-6892 group and the Cor group display notable differences in functional annotations, sig-

naling pathways, and specific biological processes. These data indicate that activation of HCAR2 results in transcriptomic alterations in microglia isolated from corticosterone-treated mice.

3.8 The Antidepressant and Neuroprotective Effects of HCAR2 Activation are Mediated by Microglia

We next investigated whether the anti-depressive and neuroprotective effects of HCAR2 activation are mediated by microglia. Mice were fed continuously with the CSF1R inhibitor PLX5622 for the entire experimental period to deplete microglia *in vivo*. AIN-76A chow was used as the vehicle control. Hematoxylin-Eosin staining (Fig. 9A) and
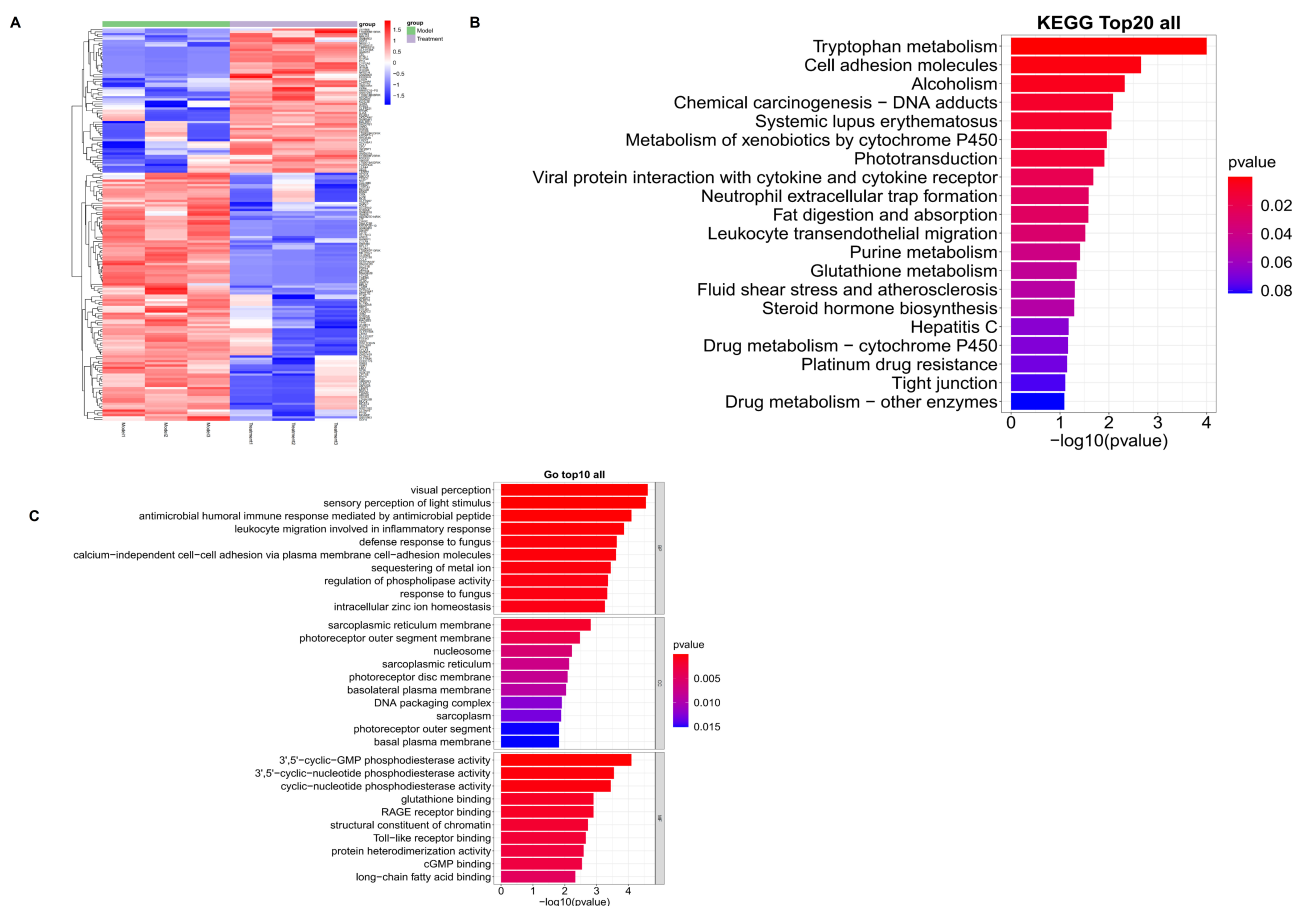
Fig. 8. HCAR2 activation induces transcriptional changes in microglial cells. (A) Heatmap plot depicting differentially expressed genes between the depression model and the MK-6892-treated depression model. (B) KEGG enrichment analysis. (C) GO enrichment analysis. KEGG, Kyoto Encyclopedia of Genes and Genomes; GO, Gene Ontology bioinformatics.

Nissl staining (Fig. 9C) revealed that microglia depletion abrogated the neuroprotective effects of MK-6892 in Cor-induced neuronal injury ($p < 0.001$, Fig. 9B; $p < 0.001$, Fig. 9D). Results from ELISA showed that microglia depletion in the Cor+MK-6892 group led to a significant reduction in the levels of 5-HT and norepinephrine (NA) (5-HT: $p = 0.037$; NA: $p = 0.013$; Fig. 9E). Moreover, the Cor+PLX+MK-6892 group exhibited significantly more depressive behaviors compared to the Cor+MK-6892 group (TST: $p = 0.029$; FST: $p = 0.002$; SPT: $p < 0.001$; OFT: $p = 0.018$; Fig. 9F). These data indicate the antidepressant and neuroprotective effects of HCAR2 activation are, at least in part, mediated by microglia.

4. Discussion

This study examined the role of HCAR2 in a corticosterone-induced mouse model of depression. Activation of HCAR2 significantly alleviated depressive-like behaviors, attenuated neuronal damage, and improved the inflammatory microenvironment. Further analysis revealed these protective effects were specifically mediated by microglia, since they were abrogated by the depletion of microglia. Moreover, HCAR2 activation led to transcriptomic changes in microglia. Our results also suggest that the AKT-IKK$\alpha\beta$-NFκB signaling pathway may play a pivotal role in this process. Microglial HCAR2 could thus be a promising therapeutic target for depression.

HCAR2, also known as GPR109A, is predominantly expressed in immune cells, adipose tissue, and the CNS. Its endogenous ligands include β-hydroxybutyric acid, nicotinic acid, and butyrate [15–18]. Emerging evidence suggests these metabolites exert antidepressant effects by promoting neurotransmitter synthesis, attenuating inflammation, and enhancing energy metabolism [19,20]. Microglia serve as the principal immune cells in the CNS, where they maintain neural homeostasis, clear cellular debris and pathogens, and play a pivotal role in neuroinflammation. Recent study has underscored the critical role of G protein-coupled receptors (GPCRs) in modulating microglial function [21]. Specifically, HCAR2 is an essential member of the GPCR family and has become a focus of research in this field. The expression of HCAR2 was significantly upregulated following microglial activation, suggesting it has a potential role in modulating microglial function [22]. The present study demonstrated that activation of HCAR2
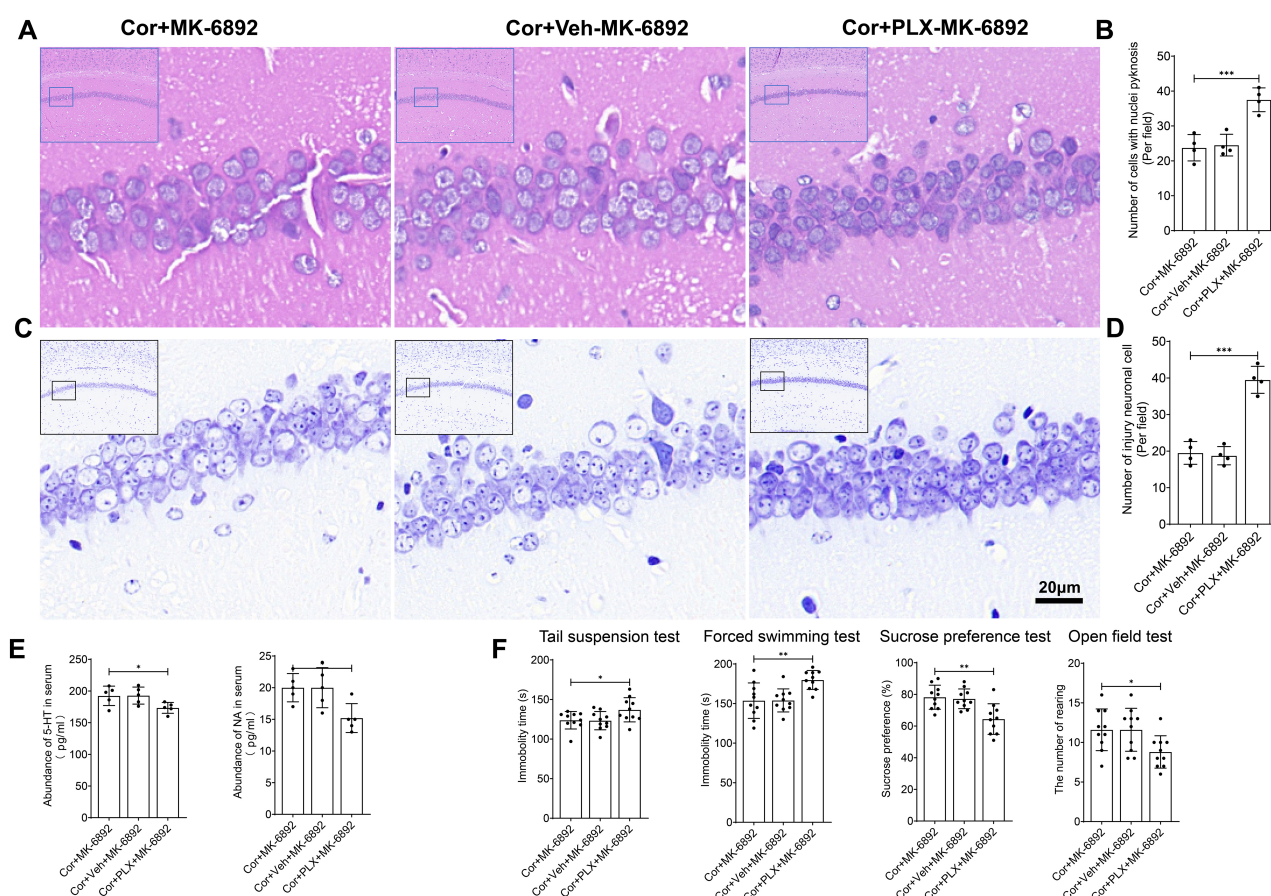
Fig. 9. The antidepressant and neuroprotective effects of HCAR2 are directly mediated through its action on microglia. (A) Representative hematoxylin-eosin stained images of the hippocampus from each experimental group. Scale bar = 20 μm. (B) Bar graph showing the number of cells with nuclear pyknosis. (C) Representative Nissl-stained images of the hippocampus from each experimental group. Scale bar = 20 μm. (D) Bar graph depicting the number of injured neurons. (E) Serum levels of monoamine neurotransmitters, as measured by ELISA. (F) Depressive-like behavior observed in each experimental group. ***$p < 0.001$, **$p < 0.01$, *$p < 0.05$. Cor, corticosterone; Veh, Vehicle; PLX, PLX5622.

significantly inhibits M1 polarization of microglia in a mouse model of depression, thereby reducing the secretion of inflammatory factors such as IL-1β, TNF-α, and IL-6. This modulation improves the inflammatory microenvironment and alleviates hippocampal injury. Moreover, our findings indicate this anti-inflammatory effect is closely linked to regulation of the AKT-IKK$\alpha\beta$-NFκB signaling pathway. Specifically, the AKT pathway acts as a central regulatory node for microglial inflammatory responses [23,24]. Upon HCAR2 activation, Gi protein signaling can inhibit PI3K/AKT phosphorylation, thereby blocking IKK$\alpha\beta$ complex activation and subsequently preventing nuclear translocation of NFκB. Since NFκB is a transcription factor for pro-inflammatory genes, its diminished activity results in decreased expression of inflammatory factors including IL-6 and IL-1β. Additionally, biased ligands of HCAR2, such as MK-6892, selectively activate the Gi pathway rather than the arrestin pathway, potentially minimizing side effects such as facial flushing and optimizing the anti-inflammatory response [25,26].

HCAR2 has been established as a critical mediator in metabolic diseases, including diabetes [27] and obesity [28], highlighting its potential influence on metabolic reprogramming. Our sequencing data revealed that activation of HCAR2 significantly alters metabolic pathways in a mouse model of depression, particularly tryptophan, purine and glutamine metabolism. An imbalance in tryptophan metabolism is a hallmark pathological feature of depression [29]. Tryptophan primarily undergoes metabolism via the kynurenine (KYN) pathway, resulting in quinolinic acid (QUIN) or 5-HT [30]. During chronic inflammation, the activity of indoleamine 2,3-dioxygenase (IDO) in microglia increases, favoring the KYN pathway and exacerbating the neurotoxic effects of QUIN on synaptic integrity [31]. Activation of HCAR2 may restore balance in tryptophan metabolism by promoting 5-HT synthesis through inhibition of microglial inflammatory responses and reduction of IDO expression. Furthermore, HCAR2 agonists may indirectly regulate tryptophan metabolism by modulating gut microbiota metabolites, such as butyrate, thereby influ-

encing the gut-brain axis. Abnormal purine metabolism is intricately associated with neuroinflammation. The extracellular accumulation of purine metabolites, such as ATP, can activate the NLRP3 inflammasome by engaging the P2X7 receptor on microglia, leading to the release of IL-1β [32,33]. Activation of HCAR2 may attenuate the ATP-induced inflammatory cascade by inhibiting purinergic receptor signaling in microglia, including signaling by P2X7. Glutamine plays a crucial role as a substrate for sustaining both the energy metabolism and immune function of microglia. During inflammation, microglia convert glutamine to glutamate via glutaminase (GLS), thereby supporting the energy demands of the pro-inflammatory phenotype through the tricarboxylic acid (TCA) cycle [34,35]. The innovation of the present study lies in its elucidation of the multi-dimensional regulatory mechanism of HCAR2 on microglia, including its effects on inflammatory signaling pathways and metabolic reprogramming. Our findings provide a robust theoretical foundation for developing anti-treatment strategies that target HCAR2. For example, niacin (Niaspan), a Food and Drug Administration (FDA)-approved HCAR2 agonist, has demonstrated efficacy in reducing neuroinflammation and improving cognitive function in models of Alzheimer's disease [22], suggesting that further investigation of its potential clinical application is warranted. Novel biased ligands, such as MK-6892, may also improve therapeutic outcomes by increasing the selectivity of Gi signaling, thereby minimizing side effects and broadening the therapeutic window. Despite significant advances in this research field, several limitations remain. Current studies rely predominantly on mouse models, which may not fully capture the species-specific expression patterns and metabolic regulation of HCAR2 in human microglia. Furthermore, the precise interaction between the AKT-IKK$\alpha\beta$-NFκB pathway and metabolic reprogramming remains incompletely understood. For instance, it is unclear whether HCAR2 influences metabolite levels by directly modulating the activity of metabolic enzymes such as IDO and GLS. This hypothesis requires further investigation at the molecular level. Another limitation is that existing research has primarily examined acute interventions, whereas long-term activation of HCAR2 could lead to receptor desensitization or compensatory mechanisms, such as overactivation of the arrestin pathway. The possibility of such effects warrants thorough assessment via long-term animal studies and rigorous clinical trials.

5. Conclusion

In summary, this study demonstrates that HCAR2 is highly effective in alleviating depressive-like behaviors and neural damage in a corticosterone-induced mouse model of depression. Mechanistically, HCAR2 activation specifically targets microglia, modulates multiple metabolic pathways, and thereby mitigates the inflammatory microenvironment, thus promoting neuroprotection. Given its role in neurochemical regulation and mood modulation, HCAR2 may serve as a promising therapeutic target for the treatment of depression.

Availability of Data and Materials

The raw sequence data reported in this paper have been deposited in the Genome Sequence Archive (Genomics, Proteomics & Bioinformatics 2021) in National Genomics Data Center (Nucleic Acids Res 2022), China National Center for Bioinformation/Beijing Institute of Genomics, Chinese Academy of Sciences (GSA: CRA026738) that are publicly accessible at https://ngdc.ncb.ac.cn/gsa. The other datasets used or analysed during the current study were available from the corresponding author on reasonable request.

Author Contributions

ZP, LJ, JCC and YJC designed the research study. ZP, LJ, JCC, SCX and YZX performed the research. ZP, PZ and YZX conducted experiments. SCX, YLY, PZ and YJC analyzed the data. ZP wrote the manuscript. All authors contributed to editorial changes in the manuscript. All authors read and approved the final manuscript. All authors have participated sufficiently in the work and agreed to be accountable for all aspects of the work.

Ethics Approval and Consent to Participate

All animal procedures were performed follow in the 3R principles and approved by the Ethics Committee of Affiliated Nanhua Hospital, University of South China (2025-KY-007).

Conflict of Interest

The authors declare no conflict of interest.

References

[1] McCarron RM, Shapiro B, Rawles J, Luo J. Depression. Annals of Internal Medicine. 2021; 174: ITC65–ITC80. https://doi.org/10.7326/AITC202105180.

[2] Souery D, Papakostas GI, Trivedi MH. Treatment-resistant depression. The Journal of Clinical Psychiatry. 2006; 67: 16–22.

[3] Penninx BWJH, Lamers F, Jansen R, Berk M, Khandaker GM, De Picker L, et al. Immuno-metabolic depression: from concept to implementation. The Lancet Regional Health. Europe. 2024; 48: 101166. https://doi.org/10.1016/j.lanepe.2024.101166.

[4] Swainson J, Reeson M, Malik U, Stefanuk I, Cummins M, Sivapalan S. Diet and depression: A systematic review of whole dietary interventions as treatment in patients with depression. Journal of Affective Disorders. 2023; 327: 270–278. https://doi.org/10.1016/j.jad.2023.01.094.

[5] Shenol A, Tenente R, Lückmann M, Frimurer TM, Schwartz TW. Multiple recent HCAR2 structures demonstrate a highly dynamic ligand binding and G protein activation mode. Nature Communications. 2024; 15: 5364. https://doi.org/10.1038/s41467-024-49536-y.

[6] Shirayama Y, Iwata M, Miyano K, Hirose Y, Oda Y, Fujita Y, et al. Infusions of beta-hydroxybutyrate, an endogenous NLRP3 inflammasome inhibitor, produce antidepressant-like effects on learned helplessness rats through BDNF-TrkB signaling and AMPA receptor activation, and strengthen learning ability. Brain Research. 2023; 1821: 148567. https://doi.org/10.1016/j.brainres.2023.148567.

[7] Qiu J, Liu R, Ma Y, Li Y, Chen Z, He H, et al. Lipopolysaccharide-Induced Depression-Like Behaviors Is Ameliorated by Sodium Butyrate via Inhibiting Neuroinflammation and Oxido-Nitrosative Stress. Pharmacology. 2020; 105: 550–560. https://doi.org/10.1159/000505132.

[8] Zhao L, Guo S, Yang J, Wang Q, Lu X. Association between niacin intake and depression: A nationwide cross-sectional study. Journal of Affective Disorders. 2023; 340: 347–354. https://doi.org/10.1016/j.jad.2023.08.053.

[9] Borst K, Dumas AA, Prinz M. Microglia: Immune and non-immune functions. Immunity. 2021; 54: 2194–2208. https://doi.org/10.1016/j.immuni.2021.09.014.

[10] Ai YW, Du Y, Chen L, Liu SH, Liu QS, Cheng Y. Brain Inflammatory Marker Abnormalities in Major Psychiatric Diseases: a Systematic Review of Postmortem Brain Studies. Molecular Neurobiology. 2023; 60: 2116–2134. https://doi.org/10.1007/s12035-022-03199-2.

[11] Pandey GN, Rizavi HS, Bhaumik R, Ren X. Innate immunity in the postmortem brain of depressed and suicide subjects: Role of Toll-like receptors. Brain, Behavior, and Immunity. 2019; 75: 101–111. https://doi.org/10.1016/j.bbi.2018.09.024.

[12] Hellmann-Regen J, Clemens V, Grözinger M, Kornhuber J, Reif A, Prvulovic D, et al. Effect of Minocycline on Depressive Symptoms in Patients With Treatment-Resistant Depression: A Randomized Clinical Trial. JAMA Network Open. 2022; 5: e2230367. https://doi.org/10.1001/jamanetworkopen.2022.30367.

[13] Bassett B, Subramaniyam S, Fan Y, Varney S, Pan H, Carneiro AMD, et al. Minocycline alleviates depression-like symptoms by rescuing decrease in neurogenesis in dorsal hippocampus via blocking microglia activation/phagocytosis. Brain, Behavior, and Immunity. 2021; 91: 519–530. https://doi.org/10.1016/j.bbi.2020.11.009.

[14] Agalave NM, Lane BT, Mody PH, Szabo-Pardi TA, Burton MD. Isolation, culture, and downstream characterization of primary microglia and astrocytes from adult rodent brain and spinal cord. Journal of Neuroscience Methods. 2020; 340: 108742. https://doi.org/10.1016/j.jneumeth.2020.108742.

[15] Nelson AB, Queathem ED, Puchalska P, Crawford PA. Metabolic Messengers: ketone bodies. Nature Metabolism. 2023; 5: 2062–2074. https://doi.org/10.1038/s42255-023-00935-3.

[16] Wuerch E, Urgoiti GR, Yong VW. The Promise of Niacin in Neurology. Neurotherapeutics: the Journal of the American Society for Experimental NeuroTherapeutics. 2023; 20: 1037–1054. https://doi.org/10.1007/s13311-023-01376-2.

[17] Zhang L, Liu C, Jiang Q, Yin Y. Butyrate in Energy Metabolism: There Is Still More to Learn. Trends in Endocrinology and Metabolism: TEM. 2021; 32: 159–169. https://doi.org/10.1016/j.tem.2020.12.003.

[18] Stilling RM, van de Wouw M, Clarke G, Stanton C, Dinan TG, Cryan JF. The neuropharmacology of butyrate: The bread and butter of the microbiota-gut-brain axis? Neurochemistry International. 2016; 99: 110–132. https://doi.org/10.1016/j.neuint.2016.06.011.

[19] Youm YH, Nguyen KY, Grant RW, Goldberg EL, Bodogai M, Kim D, et al. The ketone metabolite β-hydroxybutyrate blocks NLRP3 inflammasome-mediated inflammatory disease. Nature Medicine. 2015; 21: 263–269. https://doi.org/10.1038/nm.3804.

[20] Tian S, Wu L, Zheng H, Zhong X, Liu M, Yu X, et al. Dietary niacin intake in relation to depression among adults: a population-based study. BMC Psychiatry. 2023; 23: 678. https://doi.org/10.1186/s12888-023-05188-8.

[21] Yao H, Wang X, Chi J, Chen H, Liu Y, Yang J, et al. Exploring Novel Antidepressants Targeting G Protein-Coupled Receptors and Key Membrane Receptors Based on Molecular Structures. Molecules (Basel, Switzerland). 2024; 29: 964. https://doi.org/10.3390/molecules29050964.

[22] Moutinho M, Puntambekar SS, Tsai AP, Coronel I, Lin PB, Casali BT, et al. The niacin receptor HCAR2 modulates microglial response and limits disease progression in a mouse model of Alzheimer's disease. Science Translational Medicine. 2022; 14: eabl7634. https://doi.org/10.1126/scitranslmed.abl7634.

[23] Cai L, Gong Q, Qi L, Xu T, Suo Q, Li X, et al. ACT001 attenuates microglia-mediated neuroinflammation after traumatic brain injury via inhibiting AKT/NFκB/NLRP3 pathway. Cell Communication and Signaling: CCS. 2022; 20: 56. https://doi.org/10.1186/s12964-022-00862-y.

[24] Liao S, Wu J, Liu R, Wang S, Luo J, Yang Y, et al. A novel compound DBZ ameliorates neuroinflammation in LPS-stimulated microglia and ischemic stroke rats: Role of Akt(Ser473)/GSK3β(Ser9)-mediated Nrf2 activation. Redox Biology. 2020; 36: 101644. https://doi.org/10.1016/j.redox.2020.101644.

[25] Walters RW, Shukla AK, Kovacs JJ, Violin JD, DeWire SM, Lam CM, et al. beta-Arrestin1 mediates nicotinic acid-induced flushing, but not its antilipolytic effect, in mice. The Journal of Clinical Investigation. 2009; 119: 1312–1321. https://doi.org/10.1172/JCI36806.

[26] Yadav MK, Sarma P, Maharana J, Ganguly M, Mishra S, Zaidi N, et al. Structure-guided engineering of biased-agonism in the human niacin receptor via single amino acid substitution. Nature Communications. 2024; 15: 1939. https://doi.org/10.1038/s41467-024-46239-2.

[27] Zhang Y, Li Z, Liu X, Chen X, Zhang S, Chen Y, et al. 3-Hydroxybutyrate ameliorates insulin resistance by inhibiting PPARγ Ser273 phosphorylation in type 2 diabetic mice. Signal Transduction and Targeted Therapy. 2023; 8: 190. https://doi.org/10.1038/s41392-023-01415-6.

[28] Pan X, Ye F, Ning P, Zhang Z, Li X, Zhang B, et al. Structural insights into ligand recognition and selectivity of the human hydroxycarboxylic acid receptor HCAR2. Cell Discovery. 2023; 9: 118. https://doi.org/10.1038/s41421-023-00610-7.

[29] Correia AS, Vale N. Tryptophan Metabolism in Depression: A

Narrative Review with a Focus on Serotonin and Kynurenine Pathways. International Journal of Molecular Sciences. 2022; 23: 8493. https://doi.org/10.3390/ijms23158493.

[30] Xue C, Li G, Zheng Q, Gu X, Shi Q, Su Y, *et al*. Tryptophan metabolism in health and disease. Cell Metabolism. 2023; 35: 1304–1326. https://doi.org/10.1016/j.cmet.2023.06.004.

[31] Schwarcz R, Bruno JP, Muchowski PJ, Wu HQ. Kynurenines in the mammalian brain: when physiology meets pathology. Nature Reviews. Neuroscience. 2012; 13: 465–477. https://doi.org/10.1038/nrn3257.

[32] Peña-Altamira LE, Polazzi E, Giuliani P, Beraudi A, Massenzio F, Mengoni I, *et al*. Release of soluble and vesicular purine nucleoside phosphorylase from rat astrocytes and microglia induced by pro-inflammatory stimulation with extracellular ATP via P2X$_7$ receptors. Neurochemistry International. 2018; 115: 37–49. https://doi.org/10.1016/j.neuint.2017.10.010.

[33] Huang S, Dong W, Lin X, Xu K, Li K, Xiong S, *et al*. Disruption of the Na$^+$/K$^+$-ATPase-purinergic P2X7 receptor complex in microglia promotes stress-induced anxiety. Immunity. 2024; 57: 495–512.e11. https://doi.org/10.1016/j.immuni.2024.01.018.

[34] Andersen JV. The Glutamate/GABA-Glutamine Cycle: Insights, Updates, and Advances. Journal of Neurochemistry. 2025; 169: e70029. https://doi.org/10.1111/jnc.70029.

[35] Kalsbeek MJT, Mulder L, Yi CX. Microglia energy metabolism in metabolic disorder. Molecular and Cellular Endocrinology. 2016; 438: 27–35. https://doi.org/10.1016/j.mce.2016.09.028.